J Mater Sci (2006) 41:4678–4683
DOI 10.1007/s10853-006-0034-7

Highly surfaced polypyrrole nano-networks and nano-fibers

Muge Acik · Canan Baristiran · Gursel Sonmez

Received: 4 May 2005 / Accepted: 27 June 2005 / Published online: 4 May 2006
© Springer Science+Business Media, LLC 2006

Abstract Polypyrrole (PPy) nano-networks and nano-fibers were synthesized using interfacial and template polymerization techniques, respectively. The morphology of the PPy nano-networks showed that a homogeneous, three-dimensionally grown nano-fibers were produced. Dodecyl sulfonate was used as surfactant in the interfacial polymerization. Bulk conductivity of PPy nano-networks were in a range of 10^{-1}–10^{-4} S/cm with a surface area of ca. 480 m^2/g. Template synthesis produced one-directional alignment of conducting nano-arrays for the purpose of possible applications of these materials in charge storage devices (i.e., supercapacitors) as electrode materials. Electrochemical and spectroelectrochemical investigations showed that these materials are promising for device applications.

Introduction

The fact of having high electrical conductivities [1, 2] and spectacular film morphologies [3] in polypyrroles (PPy) make the concept of those heterocyclic conjugated polymers promising for both commercial and technological applications [4]. Following the first published report on conducting polymers in 1977 [5], PPy has been extensively studied for many applications, such as; bio- [6, 7] and gas- [8, 9] sensors, wires [10, 11], microactuators [12], coating layers [13] conductive textiles [14], solid-state devices [15], electrochromic windows and displays [16] polymeric batteries [17], electronic devices [18], functional membranes [4, 19, 20], drug and biomolecule releases [21], corrosion protections [22], and conductive adhesives [23]. Comparing to the other electroactive polymers, PPy has been alluded the researchers for proficient methods of engineering to get high-quality conducting polymers due to the nature of wide application ranges, ease of synthesis and environmental stability in the oxidized state. In these studies, one of the most widely used method for PPy synthesis is the treatment of pyrrole monomer with suitable oxidizing agents in the presence of charge-compensating dopant anions in various organic solvents or in aqueous media [1, 24, 25]. Obviously, the presence of an anionic surfactant in the reaction media is likely to improve electrical, mechanical, thermo-oxidative and hydrolytic stability due to the interaction of hydrophobic component [26]. Template-guided polymerization is another technique to produce PPy nano-fibers. Zeolites [27], alumina [28] or particle track-etched membranes [29] were used in this technique.

Recently, some major perspectives have given a chance to structure PPy thin films made of nano-fibers via interfacial polymerization. Lu et al. [30] obtained 3–4 μm PPy films by chemical oxidation of pyrrole at the interface of chloroform and water using ammonium persulfate as oxidizing agent. Lately, Zhang et al. [31] has approached to well-designed PPy nano-fibers by seeding route. In another study, large organic dopant anions such as naphthalene-sulfonic acid have contributed to PPy to proceed in a fibrillar and tubular morphology [32]. Having these related works in hand, in this study, we demonstrate three methods of synthesis to improve morphology of PPy in the presence and absence of an anionic surfactant, sodium dodecyl sulfonate.

M. Acik · C. Baristiran · G. Sonmez (✉)
Faculty of Engineering & Natural Sciences, Chemistry Program, Sabanci University, Orhanli, Tuzla, Istanbul 34956, Turkey
e-mail: sonmez@sabanciuniv.edu

Experimental

All chemicals were purchased as highly pure as possible: pyrrole (98%), chloroform (99.9%) and methanol (99.8%) (Aldrich Chemical Co.); aluminum oxide (Acros, neutral, 50–200 μ), sodium dodecyl sulfate (Sigma Chemical Co., 99%), ferric chloride (Merck Chemical Co., >98%), ammonia solution (Riedel-de Haën, 26%).

A typical interfacial polymerization reaction was performed in a 10 mL glass bottle [33]. The chloroform subphase was chosen to force the polymer formation at interface due to its immiscibility and higher density than that of water phase. A certain amount of pyrrole (0.36 mmol, 0.024 g) was dissolved in the organic phase (3 mL). Ferric chloride and sodium dodecyl sulfate were dissolved in water (18.2 Mohm, 3 mL). In a 10-mL reaction bottle, the two separately prepared phases were combined and no disturbance was allowed after mixing. In a few minutes, a thin polymer film started to form at the interface. Variations in the mol ratios of monomer, oxidant and surfactant lead us to define the optimum reaction parameters. Reactions were performed in 3 h at room temperature as the full layer formation was observed. After 3 h of polymerization, the subphase was removed and polymers were washed with 20 mL of methanol (3 times) and 20 mL of a 30% ammonia solution (3 times). The neutral polymer was centrifuged and separated from solution and dried under vacuum overnight.

Template synthesis of PPy nano-cylinders was achieved in an aqueous pyrrole (0.05 M) solution and iron (III) chloride (0.20 M) oxidant solution in water. Millipore polycarbonate membrane filters (diameter: 25 mm) with an average pore size of ca. 220 nm were sandwiched between two O-rings of a U-shaped glass tube composed of two compartments. One arm of the U-tube had a setup for holding the polycarbonate membrane. Monomer and oxidant solutions were separated with this membrane in which they diffuse through each other by the way of the pores that the polycarbonate membrane has. After successive polymerization (3 h), polycarbonate membrane was removed and washed with methanol and distilled water several times. Then the polycarbonate membrane was dissolved with chloroform remaining the polycarbonate membrane-templated PPy nano-fibers.

Morphology of PPy nano-fibers was investigated via a high resolution Supra Gemini 35 VP Scanning Electron Microscope (SEM) from Leo. Conductivity measurements were done by using Agilent 34401A 6 Digit Multimeter and interdigitated microelectrodes. A LECO, CHNS-932 instrument was used for elemental analyses measurements. The surface area was characterized via BET analyses with Micromeritics.

Electropolymerization was carried out with an Epsilon EC Potentiostat/Galvanostat, employing a platinum button (diameter: 1.6 mm; area 0.02 cm^2) or ITO-coated glass slides as working electrode, a platinum flag or wire as counter electrode, and a silver wire or 0.01 M $Ag/AgNO_3$ (Ag/Ag^+) as reference. The electrolyte used was 0.1 M of tetrabutylammonium hexafluorophosphate (Bu_4NPF_6) in water, MeCN or mixture of MeCN and water. The electrodeposition was performed from a 0.01 M solution of the monomer in the electrolyte potentiostatically at 50 mV above the oxidation potential of monomer. Cyclic voltammetry was carried out using the same electrode setup in the monomer-free electrolyte solution.

Spectroelectrochemical data were recorded on a Shimadzu UV 3150 UV–visible–NIR spectrophotometer connected to a computer. A three-electrode cell assembly was used where the working electrode was an ITO-coated glass slide ($7 \times 50 \times 0.6$ mm^3, $R_s \leq 10$ $\Omega/\square$, Delta Technologies Inc.), the counter electrode was a platinum wire and a Ag wire was used as the pseudo-reference electrode. The pseudo-reference was calibrated externally using a 5 mM solution of ferrocene (Fc/Fc^+) in the electrolyte ($E_{1/2}(Fc/Fc^+)$ = +0.130 V vs. Ag wire and +0.080 V vs. Ag/Ag^+ in 0.1 M Bu_4NPF_6/MeCN). The potentials are reported versus Ag/Ag^+. Polymer films for spectroelectrochemistry were prepared by potentiostatic deposition on ITO-coated glass slides.

Results and discussion

Interfacial polymerization is the recent fashion in synthesis of conducting polymers to get nano-structured materials [34]. Polymerization conditions obviously determine the type materials that are produced. In our system, pyrrole was polymerized with ferric chloride in the presence of a surfactant, dodecyl sulfonate (DS). Immiscible solvent system was used in which monomer and oxidizing agent were dissolved in two different solvents, namely chloroform and water, respectively. Addition of DS to the oxidant solution helps to carry the formed polymers up as a suspension in the solution. Different mole fractions of monomer, oxidizing agent and surfactant were used to optimize the resulting desired PPy structure. First the ratio of oxidizing agent to the monomer was optimized by changing the ratio from 1 to 5. Although PPys were successfully formed at the interface or at the upper layer of polymerization solution in all ratios of oxidizing agent to the monomer, a complete polymerization of pyrrole was achieved when this ratio was 3 or above, and kept as 4 for further steps. In the next step, the ratio of surfactant to the monomer was optimized by changing it in a range from 1 to 10, while keeping the mole ratio of oxidant to monomer

constant at 4. The presence of the surfactant helps the formation of suspended PPy fibers in all ratios but, the best fibrillar structures were obtained when the surfactant/monomer ratio was kept between 3 and 5.

Understanding the composition of polymer as well as the yield of polymerization is another important parameter of optimization. Polymers prepared in different time scales between 10 min and 24 h were used for calculation of percent yield and the doping level (Fig. 1). A similar trend of increase was observed in both percent yield and doping level as a function of polymerization time. At the initial stages of polymerization, a sharp increase in the yield was observed that jumped to the value of ca. 27% in 2.5 h. After this point the tendency of increase slows down. For example, the change in the yield was less than 3% between 2.5 and 5 h. Then, although an increase was seen in the yield, we believe in that this increase in yield% was resulted from the incorporation of DS to the polymer structure. This was confirmed by elemental analyses results. The DS content of polymer was determined using the ratio of S and N atoms obtained from elemental analysis that also gives doping level. A similar trend of increase in the percent yield and the doping level is an evidence for the source of the increase in yield% that is incorporated DS. Table 1 summarizes elemental analyses results for C, H, N and S atoms and the doping level calculated using the ratio of S to N atom for the PPy/DS system at different polymerization time.

Three different polymerization techniques (electrochemical, interfacial and template polymerization) were used to synthesize PPy and PPy–DS polymers. Morphologies of resulting polymers were investigated by scanning electron microscopy (SEM).

Morphology of solution side of the electrochemically prepared PPy and PPy–DS films on ITO-coated glass slides are shown in Fig. 2a and b, respectively. A three-dimensional nucleation growth was observed in both cases.

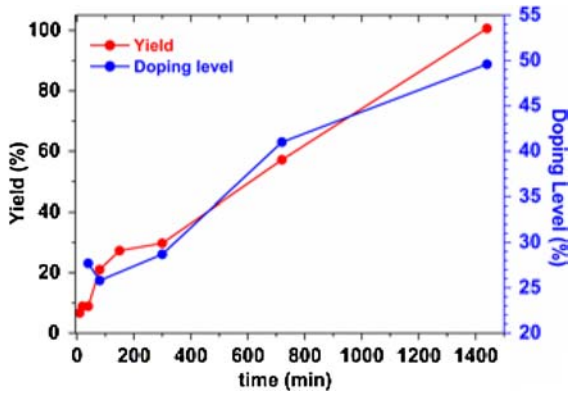

Fig. 1 Variation of the calculated percent yield and incorporation of DS to the polymer structure as a function of polymerization time

Although an irregular three-dimensional growth was observed in PPy, completely different and very regular knitting type structure was seen in the polymer films that have been grown in the presence of DS. This different nature of structure presented in Fig. 2b is very likely resulting from the steric effects induced by the long alkyl chain ended with a sulfonate dopant ion, DS. It should be noted that the same polymer films were used for spectroelectrochemistry (see Fig. 6) that will be discussed below.

In the second method interfacial polymerization technique was used in which monomer and oxidizing agent were dissolved in different immiscible solvents, chloroform and water, respectively. Pouring monomer and oxidant solutions to the same container formed two immiscible layers. Polymer films were grown starting from the interface where monomer and oxidant met each other. The surfactant DS was used to carry the formed polymers to the upper part of the solution as a suspension. It is important to note that pyyrole was only polymerized at the interface when DS was absent, resulting in a free-standing PPy films between two solution layers. Figure 3 shows the morphologies of PPys synthesized using interfacial polymerization in the presence of DS. As can be seen from Fig. 3, PPy fibers are lined with beads on them as pearl necklaces. The average diameter of fibers and beads are ca. 150 and 300 nm, respectively. The nano-fibers are homogeneously aligned in three dimensions and cross-linked after some points forming nano-networks. The presence of DS helps to form such a nano-network structure with void spaces between the fibers. The lengths of fibers, usually in a range of 1–20 μm, and the void space in between can be controlled by changing the polymerization conditions, such as concentrations of the reactants and polymerization time. A comparison of the morphology of PPy fibers at different feed ratio of surfactant to monomer is given in Fig. 3. A homogeneous network formation is clearly seen from the pictures (a) and (b) in Fig. 3 at different magnifications, in which polymers were prepared by using the surfactant/monomer ratio as 3. As the concentration of surfactant was increased to its ratio of 4 or 5 to the monomer, although the same fibrillar structure was observed, a dilution of fibers, in other words an increase in

Table 1 Elemental analyses results for C, H, N and S atoms and the doping level calculated using the ratio of S to N atom for the PPy/DS system at different polymerization time

Reaction time (min)	% C	% H	% N	% S	Doping level
40	58.00	5.30	15.46	4.31	0.28
80	64.20	5.68	15.93	4.06	0.26
300	62.28	5.61	15.67	4.54	0.29
720	60.40	6.09	13.93	5.74	0.41
1440	56.10	5.96	12.90	6.40	0.50

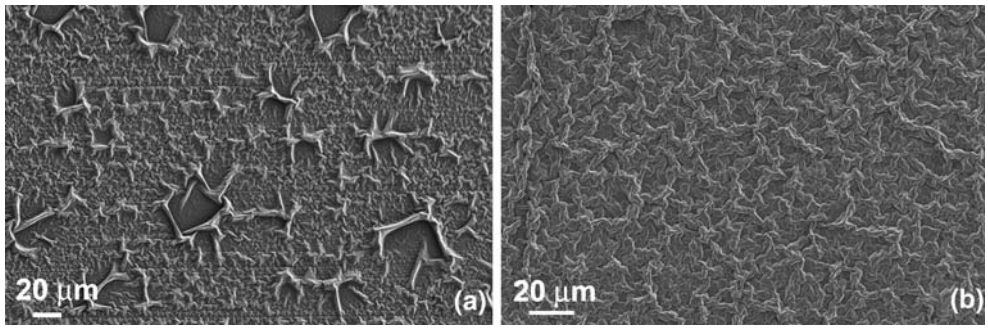

Fig. 2 SEM images of electrochemically prepared PPy films on ITO-coated glass slides (**a**) in the absence and (**b**) the presence of DS

the void spaces between fibers as well as the fiber length was observed. This different morphology obviously stems from the effect of the dilution of polymerization solution by surfactant. The surface area measured using BET technique for such structures is ca. 480 m^2/g. This very high surface area with additional nano-network structures make these materials a very good candidate for applications including gas or ion sensors [35], electrode materials for batteries, supercapacitors and fuel cells [36]. Electrical conductivity is certainly one of the most important parameter for these applications. Bulk conductivity of the nano-networked PPys ranges from 10^{-1} to 10^{-4} S/cm in the oxidized and the reduced states of polymers, respectively. It should be noted that the low conductivity values at the oxidized state may stem from the technique used and could be higher in several magnitudes of order if they were measured on a single fiber as previously reported by Martin et al. [37].

In the third method, PPy fibers were synthesized using polycarbonate membranes as template [37]. Millipore polycarbonate membrane filters (diameter: 25 mm) with an average pore size of ca. 220 nm were sandwiched between two O-rings of a U-shaped glass tube composed of two compartments. One arm of the U-tube had a setup for holding the polycarbonate membrane. Monomer and oxidant solutions were separated with this membrane in which they diffuse through each other by the way of the pores that the polycarbonate membranes have. After successive polymerization time (3 h), polycarbonate membrane was removed and washed with water several times. Then the polycarbonate membrane was dissolved with chloroform remaining in the polycarbonate membrane-templated PPy nano-fibers (Fig. 4). The dimensions of PPy nano-fibers and the void space between the fibers were determined by the pore size and the distribution of these pores in the membrane, respectively. It is important to note that depending on the polymerization time, nature of the PPy nano-fibers has shown slightly different character. For example, although the fibers obtained in a shorter polymerization time had holes inside the fibers, keeping the

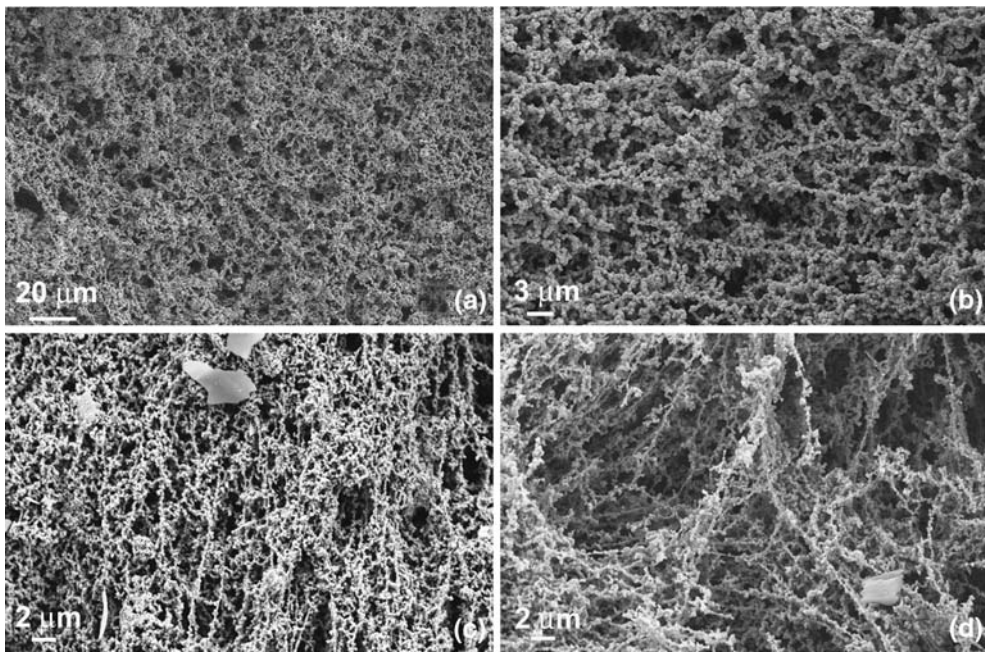

Fig. 3 SEM images of PPy nano-networks at the mol ratio of surfactant to monomer: 3 (**a** and **b**), 4 (**c**) and 5 (**d**)

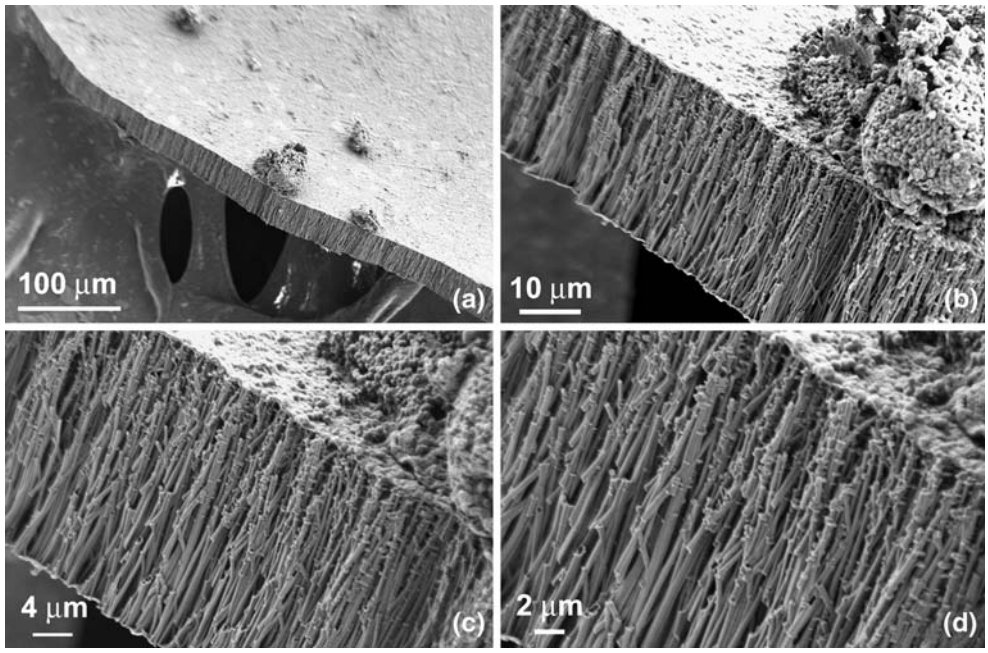

Fig. 4 SEM images of template-synthesized PPy nano-fibers at different magnifications

polymerization time longer have produced fibers without or smaller holes inside. As a result, aligned PPy nano-fibers with diameters in a range of 200–300 nm were formed. The lengths of fibers were determined by the thickness of polycarbonate membranes that was 26 μm.

PPy/DS films were potentiostatically deposited on a Pt button electrode from a solution of 0.1 M Bu_4NPF_6 in a water/MeCN (20/80) containing 0.03 M DS and 0.01 M pyrrole for electrochemical measurements. Then, polymer films were characterized by cyclic voltammetry in the monomer free electrolyte solution (Fig. 5). A linear increase in anodic and cathodic peak currents as a function of scan rate indicates that an electroactive layer is deposited on the electrode surface and the oxidation/reduction processes are not diffusion limited. The half-wave potential ($E_{1/2}$) of the polymer is about 0.0 V vs. Ag/Ag^+.

Thin PPy and PPy/DS films were deposited on ITO-coated glass substrates using potentiostatic deposition at a potential of 50 mV above the oxidation potential of pyrrole from 0.01 M monomer solution. The electrolyte used was 0.1 M Bu_4NPF_6/MeCN and a mixture of 0.03 M DS and 0.1 M Bu_4NPF_6 in a water/MeCN (20/80) for PPy and PPy/DS depositions, respectively. Figure 6 presents comparison of the spectroelectrochemistry of corresponding PPy and PPy/DS films. The π–π^* transition of both PPy and PPy/DS films displayed maxima at the edge of visible region, namely 2.95 eV (420 nm) and 3.1 eV (405 nm), respectively. The electronic band gap calculated from the onset of the π–π^* transition is 2.52 eV for PPy films. Since the π–π^* transition band for PPy/DS is not very well defined, band gap for this polymer was calculated using isobestic point resulting in almost the same value with PPy. Comparing the spectroelectrochemistry of polymer films with similar thicknesses, neutral PPy/DS has two additional absorptions at about 2.2 eV (570 nm) and 1.4 eV (900 nm) which PPy does not have. These two absorptions are most probably arisen from the incorporation of DS to the PPy films resulting in an incomplete reduction of polymer. The strong interaction between positive ions present in the polymer backbone and sulfonate groups of DS results in a reflectance at lower energies below 1.8 eV and a shoulder at 2.2 eV in the neutral polymer [38]. Upon oxidation, the π–π^* transitions are depleted at the expense of a broad band at lower energies for both polymers with slight differences. Comparing the oxidized PPy and PPy/DS films, the π–π^* transition of PPy/DS film could not be depleted completely and remained a residual absorption at 2.9 eV.

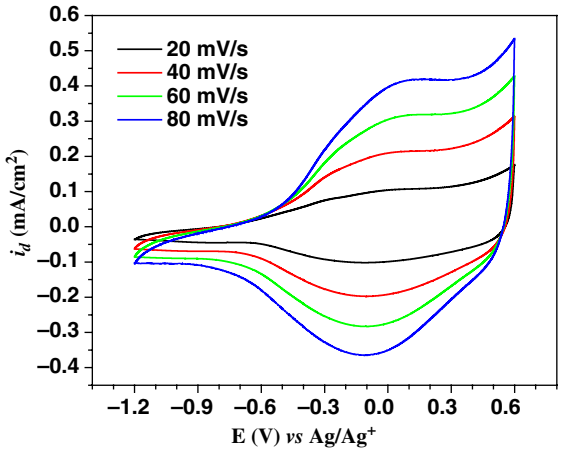

Fig. 5 Cyclic voltammetry of PPy–DS films in 0.1 M Bu_4NPF_6/MeCN at different scan rates; 20, 40, 60, 80 mV/s

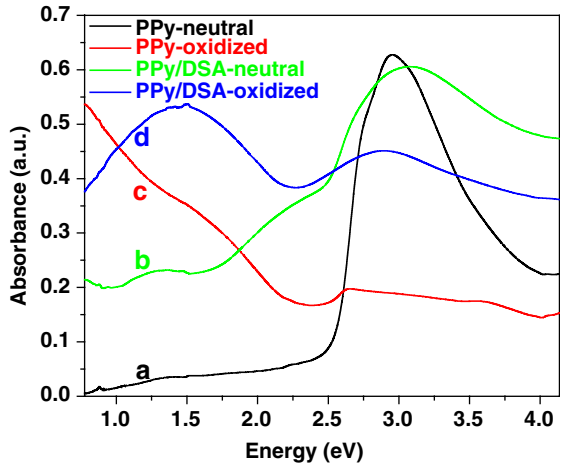

Fig. 6 Spectroelectrochemistry of PPy and PPy–DS in 0.1 M Bu_4NPF_6/PC at different oxidation states: (**a**) neutral PPy, (**b**) neutral PPy/DS, (**c**) oxidized PPy, and (**d**) oxidized PPy/DS

Similarly, the band corresponding to the intermediate energy charge carriers (radical cations) could not be converted to the low energy charge carriers (dications). A remained strong absorption at 1.5 eV might be resulted from the strong interaction of DS with PPy backbone.

In conclusion, PPy nano-networks and nano-fibers were synthesized using interfacial and template polymerization techniques. The presence of DS during the interfacial polymerization produced a homogeneous three-dimensional nano-network structure. The nano-network PPy structures obtained from interfacial polymerization had a conductivity values in a range of 10^{-1}–10^{-4} S/cm and very high surface area of ca. 480 m^2/g. To align PPy nano-fibers in one-direction polycarbonate membranes were used. One-directional alignment of these conducting nano-arrays as well as the nano-network structure was another aim of this study because of the possible applications of these materials in charge storage devices such as supercapacitors. Electrochemically synthesized PPy/DS films showed that polymer films are electroactive for applications. A combination of both Faradaic and non-Faradaic currents generated by opposite polarization of the electrodes prepared using these nano-networks and nano-arrays in a device should generate a total of huge charge due to the highly surfaced conducting polymer, which will also result in a fast charging and discharging processes. The related work will be reported in a due course.

Acknowledgements Authors gratefully acknowledge Prof. Ahmet Sirkecioglu for BET measurements. Instrumentation for this research was partially funded by TUBITAK grand TBAG-AY/104T251.

References

1. Sonmez G, Schottland P, Zong K, Reynolds JR (2001) J Mater Chem 11:289
2. Orgzall I, Lorenz B, Ting ST, Hor PH, Menon VP, Martin CR, Hochheimer HD (1996) Phys Rev B 54:6654
3. Oh KW, Park HJ, Kim SH (2004) J Appl Polym Sci 91:3659
4. Skotheim TA, Elsenbaumer RL, Reynolds JR (eds) (1998) Handbook of conducting polymers, 2nd edn. Marcel Dekker, New York
5. Shirakawa H, Lewis EJ, McDiarmid AG, Chiang CK, Heeger AJ (1977) Chem Commun 578
6. Kros A, Nolte RJM, Sommerdijk NAJM (2002) Adv Mater 14:1779
7. Ramanathan K, Bangar MA, Yun M, Chen W, Myung NV, Mulchandani A (2005) J Am Chem Soc 127:496
8. An KH, Jeong SY, Hwang HR, Lee YH (2004) Adv Mater 16:1005
9. Hosono K, Matsubara I, Murayama N, Woosuck S, Izu N (2005) Chem Mater 17:349
10. Kros A, Linhardt JG, Bowman HK, Tirrell DA (2004) Adv Mater 16:723
11. Johnson BJS, Wolf JH, Zalusky AS, Hillmyer MA (2004) Chem Mater 16:2909
12. Jager EWH, Inganäs O, Lundström I (2001) Adv Mater 13:76
13. Faverolle F, Attias AJ, Bloch B, Audebert P, Andrieux CP (1998) Chem Mater 10:740
14. Gregory RV, Kimbrell WC, Kuhn HH (1989) Synth Met 28:C823
15. White A, Slade R (2004) Macromol Symp 212:275
16. Rowley NM, Mortimer RJ (2002) Sci Prog 85:243
17. Sides CR, Martin CR (2005) Adv Mater 17:1
18. Leclerc M (1999) Adv Mater 11:1491
19. Skotheim TA (ed) (1986) Handbook of conducting polymers, vols I and II. Marcel Dekker, New York
20. Reece DA, Pringle JM, Ralph SF, Wallace GG (2005) Macromolecules 38:1616
21. Pernaut JM, Reynolds JR (2000) J Phys Chem B 104:4080
22. Stupnisek-Lisac E, Lencic D, Berkovic K (1992) Corrosion 48:924
23. Iroh JO, Su W (2002) J Appl Polym Sci 85:2757
24. Zhou XJ, Leung KT (2003) Macromolecules 36:2882
25. Mecerreyes D, Alvaro V, Cantero I, Bengoetxea M, Calvo PA, Grande H, Rodriguez J, Pomposo JA (2002) Adv Mater 14:749
26. Masalles C, Llop J, Viñas C, Teixidor F (2002) Adv Mater 14:826
27. Ikegame M, Tajima K, Aida T (2003) Angew Chem Int Ed 42:2154
28. He J, Chen W, Xu N, Li L, Li X, Xue G (2004) Appl Surf Sci 221:87
29. Martin CR (1994) Science 266:1961
30. Lu Y, Shi G, Li C, Liang Y (1998) J Appl Polym Sci 70:2169
31. Zhang X, Manohar SK (2004) J Am Chem Soc 126:12714
32. Yang Y, Liu J, Wan M (2002) Nanotechnology 13:771
33. Huang J, Kaner RB (2004) J Am Chem Soc 126:851
34. Huang J, Kaner RB (2004) Angew Chem 116:5941
35. Huang J, Virgi S, Weiller BH, Kaner RB (2003) J Am Chem Soc 125:314
36. Soudan P, Gaudet J, Guay D, Bélanger D, Schulz R (2002) Chem Mater 14:1210
37. Menon VP, Lei J, Martin CR (1996) Chem Mater 8:2382
38. Sonmez G, Sarac AS (2002) J Mater Sci 37:4609